Results in Engineering 28 (2025) 106914

Contents lists available at ScienceDirect

Results in Engineering

journal homepage: www.sciencedirect.com/journal/results-in-engineering

Research paper

Physics-informed computational framework for assessing the seismic behavior of the Prince Moulay Abdellah Dam

Cecilia Rinaldi [a,1], Amine Bendarma [b,1], Francesco Potenza [c,*,1], Vincenzo Gattulli [a,1]

[a] Department of Structural and Geotechnical Engineering, Sapienza University of Rome, via Eudossiana, 18, Rome, 00184, Italy
[b] Arts et Métiers Campus de Rabat, Parc Technopolis, Rocade de Rabat-Salé, Campus UM6P, Sala Al Jadida, 11100, Morocco
[c] Department of Engineering and Geology, University "G. d'Annunzio" of Chieti-Pescara, V.le Pindaro 42, Pescara, 65127, Italy

ARTICLE INFO

Keywords:
Digital twin
BIM-FEM interoperability
Dam monitoring
Prince Moulay Abdellah Dam
Marrakech-Safi Eartquake

ABSTRACT

Dams in seismically active regions require rigorous structural assessment to ensure safety and protect downstream communities. To address this challenge, the present study integrates Building Information Modeling (BIM), Finite Element Method (FEM) modeling, and real-time structural health monitoring into a novel framework for seismic evaluation of the Prince Moulay Abdellah Dam in the Agadir region of Morocco. A detailed BIM-based digital replica of the dam was developed to ensure seamless interoperability with FEM simulations and incorporation of on-site sensor data. This integrated approach captured different displacement patterns during the magnitude 6.8 earthquake on September 8, 2023. The dam abutments experienced noticeable increases in longitudinal displacement, while the central vault remained largely stable. The FEM analysis corroborated the field measurements, indicating that critical structural elements (for example, concrete block joints) remained within acceptable stress limits, thus preserving the structural integrity of the dam during the event. These results demonstrate the effectiveness of combining BIM, advanced numerical modeling, and real-time monitoring in accurately characterizing dam behavior under seismic loading. The findings underscore the value of such an integrated digital modeling strategy for improving dam seismic safety and resilience, informing predictive modeling of future performance, and guiding proactive risk management in dam safety and seismic risk assessment.

1. Introduction

The structural integrity and maintenance of dams are critical due to their essential role in water resource management, irrigation, and flood protection. Failure in such infrastructure can have severe social and economic consequences. Throughout their service life, dams are exposed to a combination of operational and environmental loads, including seismic activity, hydrodynamic forces, temperature fluctuations, and material degradation due to creep and shrinkage. Consequently, data-driven health monitoring has become a fundamental approach to early detection of anomalies and risk mitigation in dam safety programs [1,2].

International dam safety protocols require periodic structural evaluations through a combination of full-scale reviews every five to twenty years, post-event inspections following extreme occurrences such as earthquakes and floods, and frequent safety checks, typically on an annual or even weekly basis [3]. Regular monitoring data are collected and analyzed based on predefined trend patterns, which requires automated processing for efficient anomaly detection. Advanced monitoring techniques, such as accelerometer-based dynamic structural assessments, have been successfully implemented in arch dams, enabling the continuous characterization of modal properties during reservoir filling and structural loading variations [4]. Furthermore, methodologies that integrate automatic data analysis with computational three-dimensional finite element models have proven effective in simulating the dynamic behavior of dams, supporting predictive assessments of stress and displacement distributions [5,6].

The Finite Element Method has become a standard approach in dam engineering, aiding in both the design of new structures and the assessment of existing ones [7,8]. Validating numerical simulations against in situ monitoring data remains essential to ensure accuracy in predicting structural responses [9–13]. Studies utilizing forced vibration

* Corresponding author.
E-mail addresses: cecilia.rinaldi@uniroma1.it (C. Rinaldi), amine.bendarma@gmail.com (A. Bendarma), francesco.potenza@unich.it (F. Potenza), vincenzo.gattulli@uniroma1.it (V. Gattulli).
[1] These authors contributed equally to this work.

https://doi.org/10.1016/j.rineng.2025.106914
Received 9 June 2025; Received in revised form 8 August 2025; Accepted 22 August 2025

Available online 3 September 2025

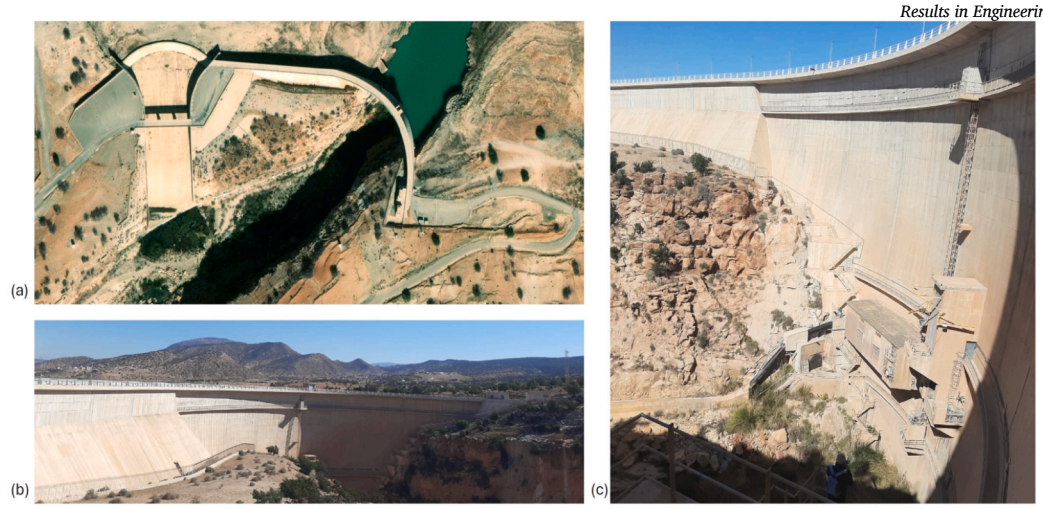

Fig. 1. The Moulay Abdellah Dam in the Souss-Massa region, Morocco: (a) aerial view, (b) lateral view downstream, (c) detailed downstream section.

tests have demonstrated the potential of experimental methodologies in characterizing the dynamic response of dams, enabling real-time assessment of their structural conditions [14,15]. In addition, Artificial Neural Networks (ANN) and machine learning procedures have emerged as promising tools for processing heterogeneous monitoring datasets, identifying structural damage features, and predicting long-term deformation trends [16–18], and, recently, also for improving the seismic demand prediction [19,20]. Recently, information on the real conditions of structures, infrastructure, and dams has been improving using satellite measurements [21,22].

Despite advances in monitoring and numerical modeling, dam assessment remains hampered by fragmented data sources and a lack of integrated analysis frameworks. The Digital Twin paradigm, which merges real-time sensor data with digital models, offers a solution by linking dynamic monitoring information with static geometrical and structural attributes stored in Building Information Modeling (BIM) systems [23,24]. Initially developed for the architectural and construction industries, BIM technology has gained prominence in civil engineering and infrastructure management, providing enhanced interoperability, visualization, and automated data integration capabilities [25]. Recently, this methodology has been applied to historical buildings (HBIM, Historic BIM), for damage mapping and monitoring, and performing energy analysis [26,27]. In addition, Industry Foundation Classes (IFC) standards facilitate seamless data exchange between engineering disciplines, ensuring accurate representation of structural components and performance indicators. IFC is an open, neutral data standard that is appropriately structured for exchanging information among different aspects of a building—structural, energy-related, maintenance, and so on. From a structural-analysis perspective, an interesting methodology was presented in [28]. In that study, the authors developed an automatic tool that generates a tetrahedral mesh while simultaneously assigning mechanical properties—such as self-weight and fixed base constraints—directly from the OpenBIM (IFC) data.

This study focuses on integrating BIM and FEM methodologies [29] to analyze the seismic response of the Prince Moulay Abdellah Dam, located in the Agadir region of Morocco, an area characterized by high seismic activity. The dam plays a pivotal role in regional water resource management, irrigation, and flood mitigation, necessitating robust structural assessments to ensure its long-term resilience [30]. The September 8, 2023, magnitude 6.8 earthquake provided an opportunity to assess the real-time response of the dam, analyzing displacement trends and stress distributions captured by its structural health monitoring system. By integrating geotechnical, hydrological, and structural data, this study identifies critical structural vulnerabilities and offers insights for defining preventive maintenance strategies and seismic risk mitigation measures [31,32].

Using recent advances in BIM-enabled seismic analysis, this research demonstrates how the interoperability between numerical modeling and real-time monitoring improves the accuracy and efficiency of dam performance assessments [33]. The findings contribute to the broader adoption of digital twins and BIM-driven predictive modeling in dam engineering, advocating for resilient infrastructure design and proactive risk management.

2. The Moulay Abdellah Dam

The Moulay Abdellah Dam (Fig. 1) was constructed between 1999 and 2002 and is located approximately 60 km from Agadir, Morocco, in the Souss-Massa region. Designed to support regional water resource management, the dam plays a crucial role in ensuring water supply, irrigation, and flood control for Agadir and surrounding areas.

Structurally, the dam is a reinforced concrete double curvature arch designed to efficiently transfer external loads to the adjacent rock abutments. This design minimizes the amount of reinforced concrete required compared to single-curved arch dams, while still ensuring structural stability. The dam has a thickness varying between 7 meters, at the base, and 2.5 meters, on the top, and extends for 166 meters along the bridge, reaching a maximum height of 65 meters from the foundation. The reservoir generates a storage capacity of 110,000 cubic meters and regulates an annual water volume of 27,500 cubic meters.

The structural performance of the dam is influenced by several interacting forces, including the hydrostatic pressure exerted by the reservoir, the uplift water pressure at the foundation, and the self-weight of the dam body. Environmental factors such as temperature variations, chemical reactions, and material aging also affect its behavior over time. Additionally, external loads from seismic activity, floods, and sediment accumulation contribute to the dam's overall stability challenges. Ensuring long-term structural integrity requires continuous Structural Health Monitoring (SHM) to detect early warning signs of potential failure mechanisms.

To achieve this, the Moulay Abdellah Dam is equipped with an advanced monitoring system that collects real-time data on structural and environmental conditions. Three strain gauges, located on the right shoulder, right bank, left bank, and valley bottom, measure deformations in the body of the dam. The displacement monitoring system includes direct and reverse pendulums, installed in three dedicated chambers, to track horizontal movements, and a vinchon-based displacement measurement system, based on the use of 17 winches, installed across the dam joints on the crest and on the abutments to monitor the opening of the joint. Two accelerographs, located at the crest and left bank, record seismic activity and structural vibrations. Additionally, two flow meters on each side of the dam monitor soil permeability losses and

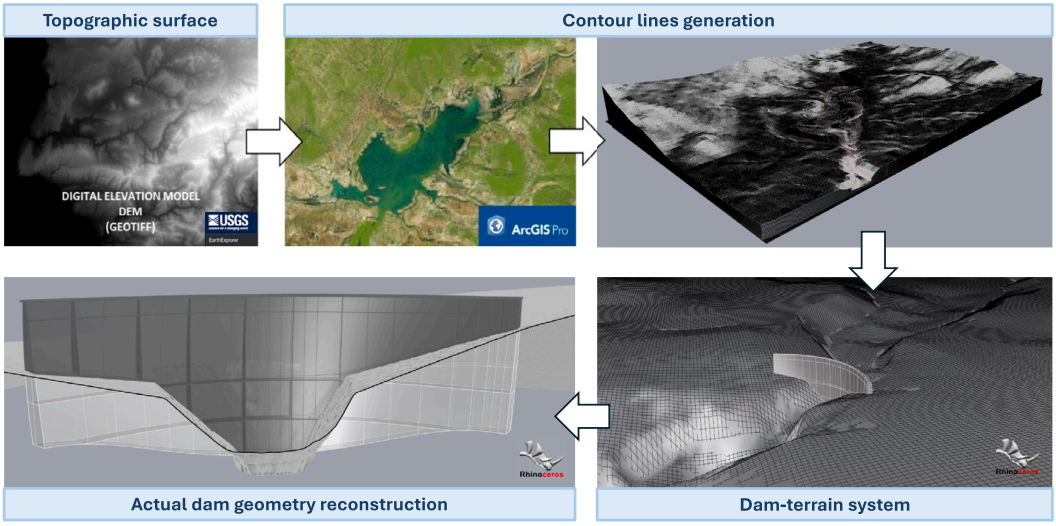

Fig. 2. Geometry reconstruction of the dam-terrain system through the evaluation of the topographic surface.

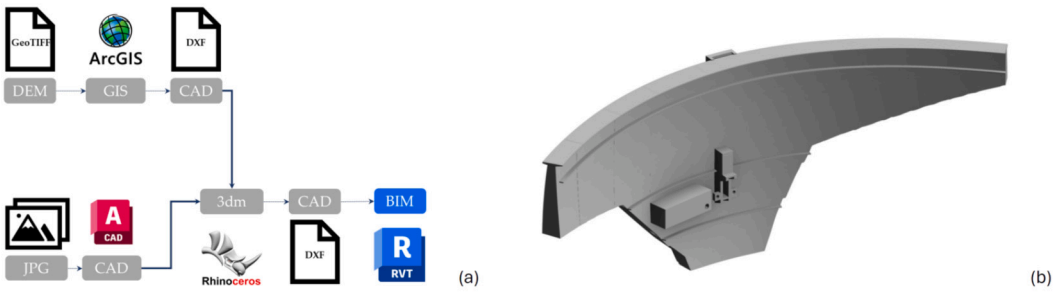

Fig. 3. BIM modeling: (a) Workflow of the BIM-GIS integration for geometry reconstruction and geolocalization, (b) BIM model of the vault of the dam.

overall stability. Thermal behavior is assessed through five temperature sensors and thermocouples embedded in the main body of the dam, providing insight into daily and seasonal temperature variations. In addition, six piezometers are installed in the central section of the dam, measuring both the water pressure and the lift pressure in the foundation. These monitoring instruments provide a continuous stream of data, allowing engineers to assess real-time structural conditions, track trends, and implement preventive maintenance measures.

A centralized digital platform has been used to manage and analyze the data collected from the dam monitoring system. This system integrates multiple sources of information, including design documentation, real-time monitoring data, maintenance reports, and inspection records, providing a comprehensive overview of the operational status and structural health of the dam. The platform is designed to systematically organize and securely store information, allowing engineers and maintenance teams to access relevant data efficiently. Through an interactive interface, specialists can analyze trends, identify anomalies, and make informed decisions on necessary interventions. In addition to real-time monitoring, the system includes maintenance management functionalities, enabling the scheduling of inspections, logging of repairs, and tracking of the lifecycle of dam components. By consolidating all relevant data, this platform enhances coordination among different teams, streamlines maintenance operations, and ensures a proactive approach to risk management.

The integration of structural monitoring with digital data management represents a significant advancement in the long-term resilience of the Moulay Abdellah Dam. By combining real-time sensor data with engineering analysis, the system enables a comprehensive and data-driven approach to dam safety, structural performance evaluation, and disaster mitigation strategies.

3. Dam modeling

3.1. BIM-FEM interoperability

To simulate the mechanical behavior of the dam's main barrier element, a FEM model was developed by leveraging interoperability with BIM environment. A BIM model of the dam was created using technical design documentation, while the Earth Explorer platform was utilized to enhance the geometry reconstruction of the dam-terrain system. The topographic surface was derived from Digital Elevation Model (DEM) data, which contains information about the site's altimetric dimensions. These data, obtained from EarthExplorer4F5, incorporate satellite imagery, aerial photographs, elevation datasets, land cover information, and digitized maps. By importing the DEM file into a Geographic Information System (GIS) environment, the site's contour lines were generated (Fig. 2). The actual dam geometry was reconstructed by intersecting the curved solid model with the topographic surface in Rhinoceros software.

The BIM model (Fig. 3) was finalized to include detailed information on the monitoring system and sensor data. Managing this information within a BIM framework enables efficient visualization of the sensor layout and facilitates easy access to real-time SHM data. Each monitoring sensor was modeled based on its actual geometry and position (Fig. 4a), and a set of unique entities was assigned to store metadata, including sensor type, manufacturer details, installation date, measured physical parameters, identification codes, and maintenance records (Fig. 4b).

This digital modeling process, complemented by machine learning-based automation, facilitates the development of a digital twin of the dam. The digital twin enables real-time infrastructure monitoring, supporting early detection of structural anomalies, damage assessment, and predictive maintenance. Integrating 3D modeling, visualization tools,

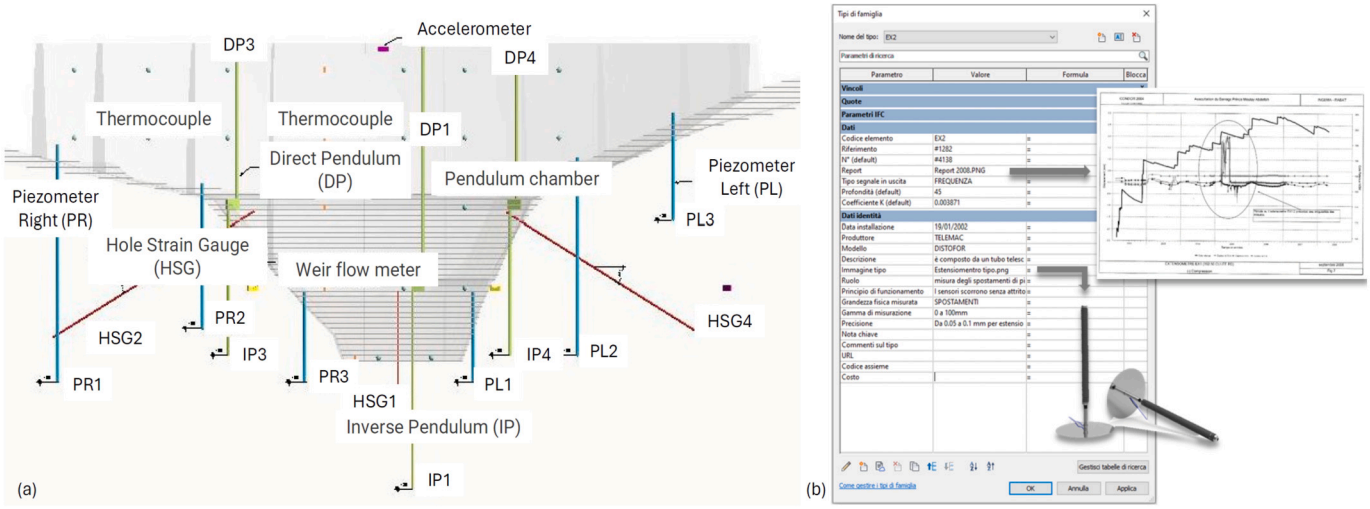

Fig. 4. BIM modeling of monitoring system: (a) sensor layout, (b) example of monitoring information linked to one sensor.

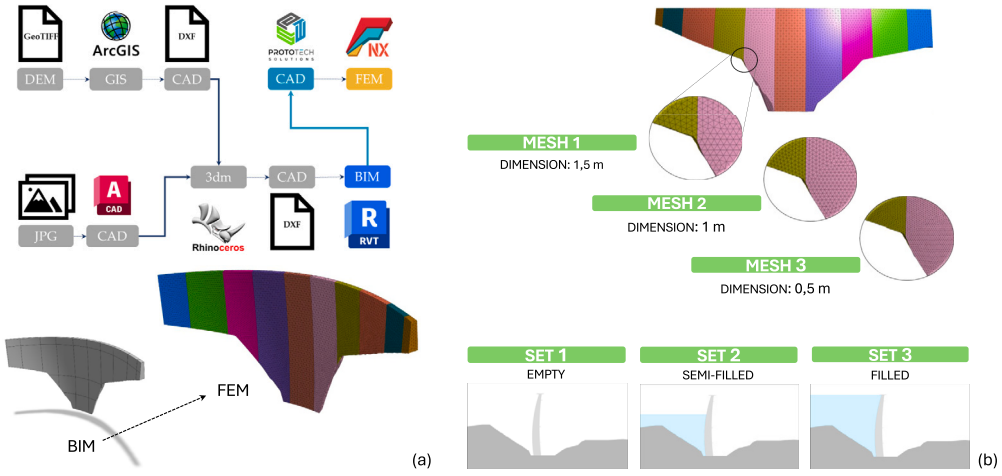

Fig. 5. BIM-FEM interoperability: (a) BIM-FEM integration for 3D elements modeling, (b) FEM modeling: mesh size of the 3D elements and reservoir filling scenarios.

and structured data management significantly enhances the ability to assess dam performance and streamline maintenance operations.

The BIM model was seamlessly integrated with the FEM environment (Fig. 5a) using the PARASOLID Exporter for Revit plug-in (ProtoTech Solutions). The Parasolid format (.x_t / .x_b), developed by Siemens, is widely used for representing complex 3D geometries and surfaces with high precision. The text-based .x_t format is human-readable, while the binary .x_b format is more compact and faster to process. Its robustness in preserving geometry, topology, and tolerance makes it ideal for high-fidelity engineering applications, including BIM-to-FEM conversion, where complex geometries like those in dam structures are maintained. The plugin facilitates direct export from Revit to FEM formats, preserving key data such as geometry, material properties, and geolocation. For dam modeling, the process involves the following steps:

- Geometry Export: The 3D geometry of the dam (e.g., cross-sections, superstructures, tunnels) is exported in Parasolid format, preserving complex shapes and dimensions for accurate simulation of hydraulic and structural behavior.
- Material and Structural Properties Mapping: Material properties like density and elasticity are automatically transferred from Revit to the FEM model. This includes specific materials like concrete, steel, and geotechnical materials, ensuring proper assignment in the FEM model.
- Geolocation Integration: Geographic coordinates and site-specific data are transferred to accurately align the model with its physical location, which is crucial for dam modeling due to its dependence on terrain and water interaction.
- Mesh Generation and Analysis Setup: The FEM software generates the mesh. For dams, it is essential to consider a mesh that can capture details such as pressure variations along the dam wall and torsional forces caused by hydraulic stresses. Boundary conditions and load cases are then defined based on project requirements, including both static and dynamic loads, such as those due to reservoir filling and seismic forces.

This integration eliminates manual steps, ensuring the BIM model's accuracy when transitioning to FEM, enabling precise analysis of the dam's interaction with terrain and water.

A finite element analysis was conducted, focusing on the effects of the mesh size and the reservoir filling level. The study examined the modal analysis results considering three different mesh resolutions (1.5 m, 1.0 m, 0.5 m), each simulated under three reservoir filling conditions (empty, semi-filled, filled) as shown in Fig. 5b.

The analysis aims to evaluate the variation of the natural frequencies concerning changes in reservoir water levels and mesh size. As shown in Fig. 6, the natural frequencies increase as the level of the reservoir decreases, due to the reduction of the participating mass. A slight decrease in frequencies is observed as the mesh size decreases, indicating

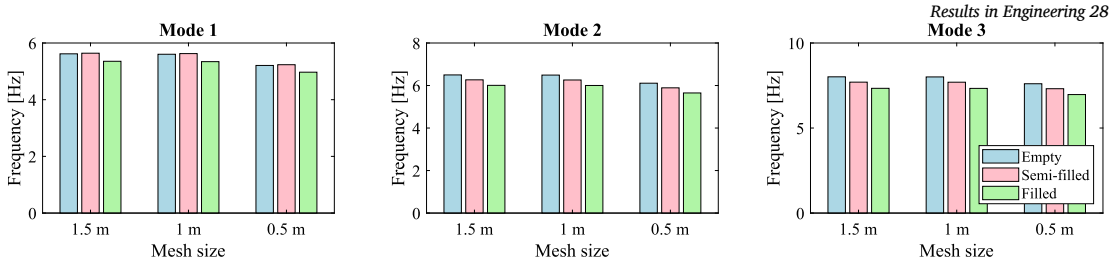

Fig. 6. Natural frequencies of the first 3 modes as a function of the mesh size and the reservoir level (Set 1, Set 2, Set 3).

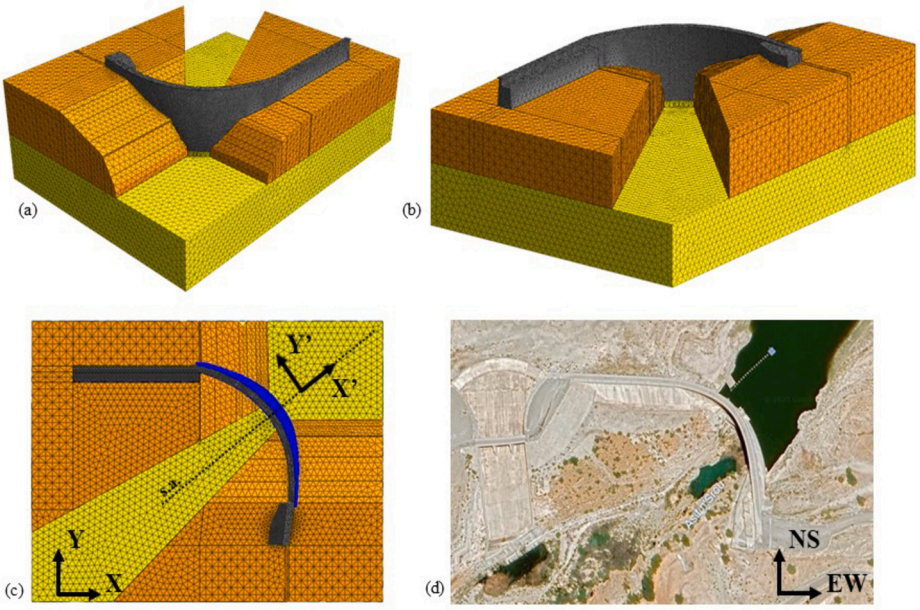

Fig. 7. 3D model representative of the interaction soil-structure: (a) and (b) 3D views, (c) view from above, (d) satellite view. In image (c) the directions of the reference system oriented concerning the symmetric axis (s.a.) have also been indicated (X' and Y').

the influence of mesh refinement on the accuracy of the model. This result confirms that the mesh has reached an acceptable level of convergence. For the three mesh resolutions, the finite-element model with a 1.5 m element size contains 52,675 elements and 12,851 nodes; the 1.0 m mesh comprises 174,186 elements and 36,943 nodes; and the finest mesh, with 0.5 m elements, consists of 1,391,322 elements linked by 266,233 nodes. All models were developed in MIDAS FEA NX, using solid tetrahedral elements to simulate the dam's structural behavior.

Additional methodologies were investigated to enhance the integration between BIM and FEM model. Within the BIM framework, a reference surface intersecting the centroids of the principal dam sections was generated using the "mass" function and subsequently imported into the FEM platform for two-dimensional finite element analysis. During the meshing phase, surface discontinuities were identified and rectified by implementing high-resolution point grids, developed via visual programming scripts. Although 2D-based FEM models provide notable computational efficiency, they require manual calibration to accurately represent the variation in plate thickness along the vertical profile of the dam.

3.2. Soil-structure interaction modeling

To better describe the interaction between soil and structure, a 3D FEM model has been implemented in Midas FEA NX software. In Fig. 7a,b are reported two 3D views of such model. Given the low level of knowledge about the territory's morphology, the river bed and the right and left banks have been obtained through extrusion and geometric operations. Based on the experimental geological surveys (made nearby the dam), the typologies of the soil can be grouped into two categories: (1) peliti soil (yellow layer in Fig. 7a,b) and dolomitic limestones (orange layer in Fig. 7a,b). The linear and elastic parameters describing the constitutive laws of these two soils have been selected based on the values found in the literature ([34,35]). In particular, the peliti and dolomitic limestones have been assimilated into siltstone and limestones, respectively. The parameters chosen in terms of elastic modulus, Poisson coefficients, and weights per unit of volume for the soil materials and dam (reinforced concrete, gray color in Fig. 7a,b) have been reported in Table 1. The boundary conditions have been inserted on the soil base and have been modeled as hinges. Figs. 7c and Figs. 7d show how the global X-direction of the model corresponds, substantially, to the East-West EW-direction and, consequently, the Y-direction to the North-South NS-direction. In total, the model is composed by 278,778 tetrahedral elements linked together by 58,097 nodes.

Table 1
Definition of the elastic constitutive laws for the materials of the 3D model related to the interaction soil-structure (Fig. 8a,b).

Type of material	Elastic modulus [MPa]	Poisson Coefficient [-]	Weight [KN/m^3]
Reinforced concrete	31,000	0.20	24.00
Peliti (siltstones)	65,000	0.25	25.50
Dolomitic Limestones	50,000	0.25	24.00

Similarly to the previous case, three distinct structural configurations were developed to perform the modal analysis. They are related to the conditions of the reservoir that can be: (1) empty, (2) partially (semi-) filled (about 42 m, 70% of the filled configuration), and (3) filled (about 60 m). The different phases of filling in the 3D model are illus-

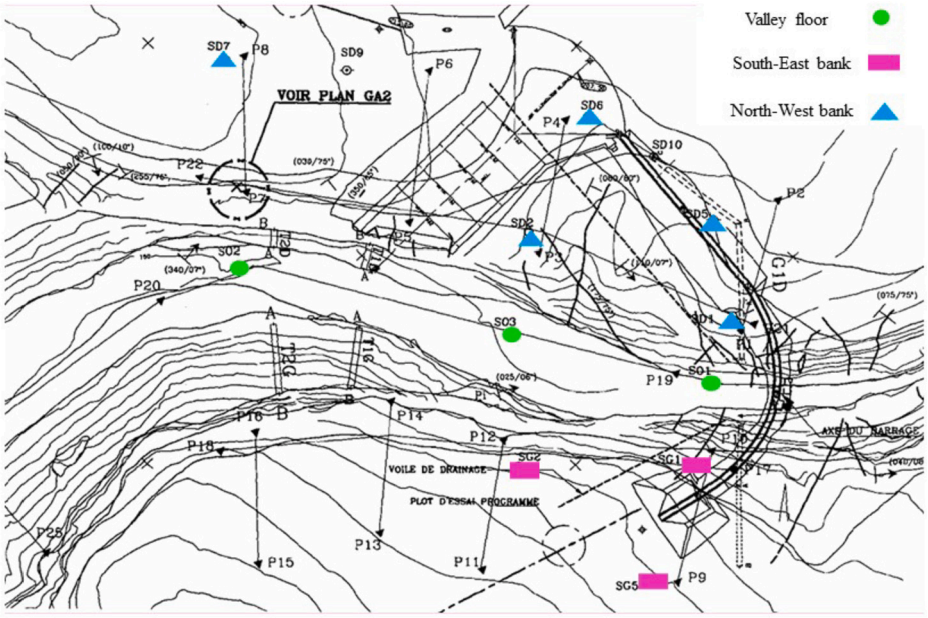

Fig. 8. Location of the cores drilling useful to identify the type and the depth of the soil on the valley floor, south-east and north-west bank of the river.

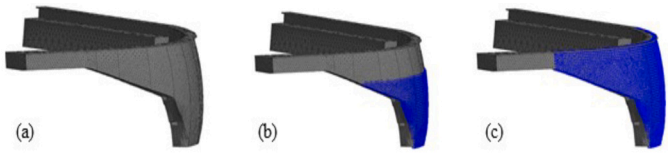

Fig. 9. Three different configurations related to the condition of the river: (a) empty, (b) partially filled, (c) filled.

Table 2
The first four modal frequencies for the different configurations, [Hz].

Configurations	First mode	Second mode	Third mode	Fourth mode
Empty	5.667	6.428	6.600	7.200
Partially filled	5.647	6.420	6.599	7.200
Filled	5.252	6.048	6.582	7.190

trated in Fig. 9. The presence of the water has been applied to the dam by a static pressure load as visible by the blue color of Figs. 9b,c, that, substantially, corresponds to an increase of mass. The frequencies for the empty and partially filled configurations are very near each other, while they become more flexible in the case of filled scenarios (Table 2). Moreover, in the first two cases, the second and third frequencies are very close to each other, while they become well-separated in the third case. The modal shapes are similar looking at the different configurations (Fig. 10). The modes show the following deformed shapes: the first and second are symmetric and anti-symmetric concerning the symmetric axis of the dam, respectively, (see Fig. 7c), while the third and fourth are symmetric, with the fourth showing a higher degree of symmetry. It is important to emphasize the influence of water presence on the modal characteristics. This effect is particularly noticeable in the fourth mode of the filled reservoir configuration (Fig. 10c), which exhibits a higher degree of symmetry compared to the corresponding mode in the empty-reservoir condition.

Such 3D FEM model is beneficial to design a seismic structural health monitoring system. Indeed, a simple response spectrum analysis can provide important information about the position of a minimum number of accelerometers. To define an elastic spectrum, chosen as a reasonable input, the NTC Italian technical rules have been referred to (Fig. 11b). In particular, the selection of the parameters required by the code and necessary for the implementation of the response spectrum was based taken into account the seismic ground acceleration map of Morocco, as shown in Fig. 11b. It shows that the Moulay Abdellah Dam is located in a zone with high seismicity. For this reason, the spectrum has been defined by selecting a city in central Italy (Campotosto, Abruzzo region), with approximately the same seismicity, and where another dam has been realized. Other parameters used have been the following: nominal life 50 years, use category 2, reference period 100 years, soil and topography category A and T3, respectively.

Subsequently, a seismic response spectrum analysis was performed using the previously described input, reducing it to achieve a maximum accelerometric structural response equal to 0.5 g. Four spectrum directions were selected: two in X and Y directions (EW and NS, respectively) and the other two along the symmetric axis of the dam, X', and in its perpendicular direction, Y'. They have been highlighted in Fig. 7c. In Fig. 12a,b, as an example, the percentage of the distributions of the accelerations has been reported for the X'- and Y-spectrum directions. In particular, the first input (X'-direction) shows the maximum acceleration response equal to about 0.50 g, and it is located at about a quarter of the dam length. The analysis of the Y-direction input demonstrates that the peak acceleration shifts toward the center of the dam. The results in the other directions provide maximum accelerations below the ones observed in X'-direction. Moreover, their locations have always been found at a quarter, three-quarters, and half of the dam's length. Such linear seismic analysis has been performed for both empty and filled configurations, while the coefficient of reduction of the original spectrum is equal to 0.08. Now, it is opportune to verify the corresponding tensions found under these four spectrum directions. The focus has been paid to the normal tensions: $\sigma_{x,x}$, $\sigma_{y,y}$, $\sigma_{z,z}$. In Fig. 12c and d, the tensions in the z-direction related to the seismic spectrum in X'- and Y-direction have been illustrated. They are mainly compression, and the maximum values are -0.67 MPa and -0.88 MPa, respectively. The whole scenario is reported in Table 3 for the empty and filled cases. In these Tables are illustrated the range of tensions mainly distributed in all directions, for the spectrum directions examined. Corresponding to these ranges is the percentage of distribution on the structure. The maximum tensions have been found for the filled case in the z-direction. They assume the values of -0.96 MPa for compression and 2.17 MPa for tensile. Moreover, for each case, the maximum accelerations are also reported, all below 0.50 g as found in X' spectrum's direction.

Another check has been carried out on the material working rate. It is substantially a comparison of the maximum compression and tensile

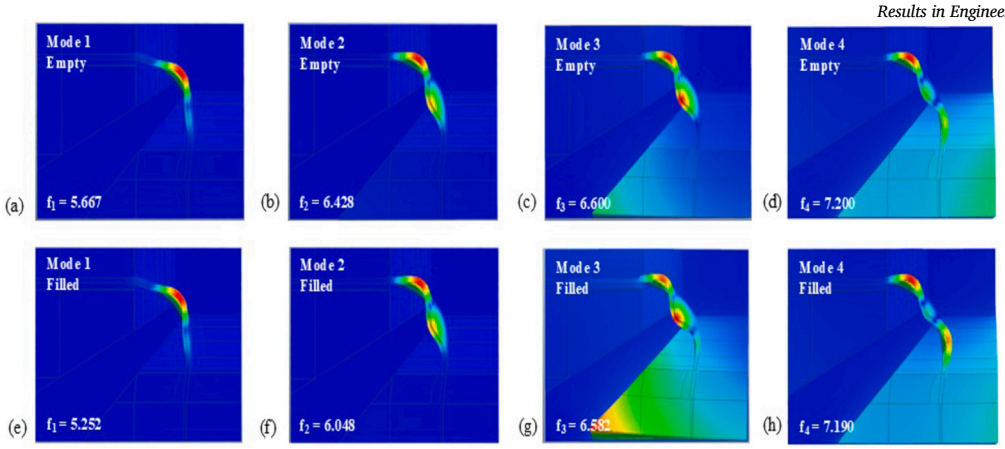

Fig. 10. The first four modes related to the empty and filled configurations involving predominantly the dam.

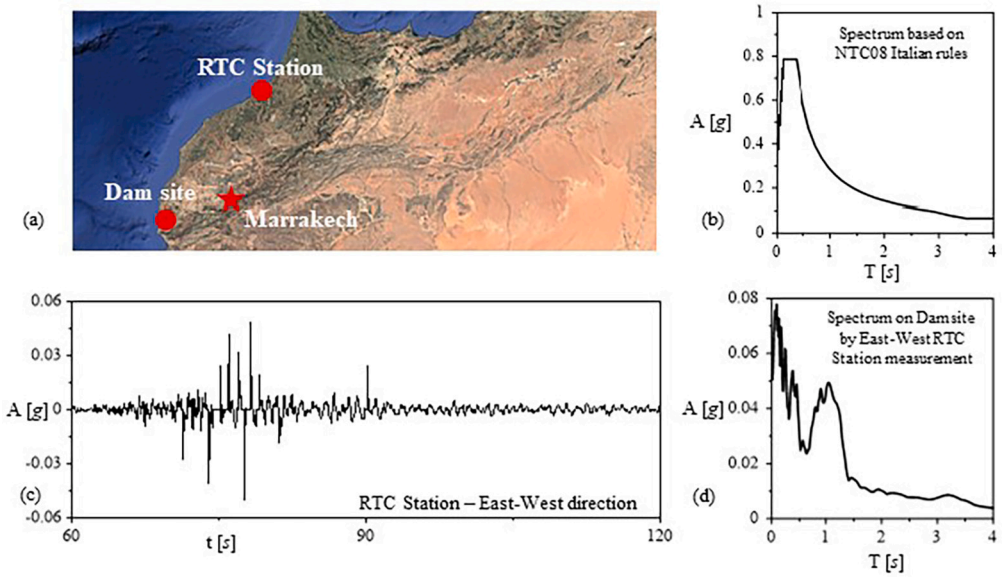

Fig. 11. (a) Locations of the RTC Station (http://terremoti.ingv.it/instruments/station/RTC), Marrakesh (epicenter) and dam site. (b) Spectrum based on NTC08 Italian rules. (c) Ground acceleration (East-West direction) recorded by the RTC Station. (d) Spectrum on sam site by RTC Station measurement.

Table 3
Maximum accelerations and range of the normal tensions mainly distributed for different spectrum directions.

Conf.	Spec. dir.	Max Acc. [g]	$\sigma_{x,x}$ [MPa]		$\sigma_{y,y}$ [MPa]		$\sigma_{z,z}$ [MPa]	
			Range	(%)	Range	(%)	Range	(%)
Empty	X	0.39	-0.43 ÷ +0.07	87.6	-0.21 ÷ +0.03	68.0	-0.59 ÷ +1.03	100
	Y	0.40	-0.57 ÷ +0.10	94.5	-0.06 ÷ +0.40	60.9	-0.88 ÷ +1.76	100
	X'	0.46	-0.03 ÷ +0.70	84.1	-0.13 ÷ +0.29	84.9	-0.62 ÷ +2.09	100
	Y'	0.33	-0.30 ÷ +0.31	100	-0.07 ÷ +0.33	59.8	-0.95 ÷ +0.55	100
Filled	X	0.41	-0.48 ÷ +0.07	83.3	-0.11 ÷ +0.16	89.2	-0.60 ÷ +1.36	100
	Y	0.36	-0.19 ÷ +0.42	97.5	-0.07 ÷ +0.23	62.8	-0.30 ÷ +2.17	100
	X'	0.50	-0.01 ÷ +0.73	72.2	-0.12 ÷ +0.32	84.6	-0.67 ÷ +2.16	100
	Y'	0.25	-0.26 ÷ +0.26	100	-0.08 ÷ +0.12	69.4	-0.96 ÷ +0.48	100

tensions with the admissible ones. The latter can be calculated using formulas widely used in technical literature. They are reported in the following equations:

$$\sigma_{adm,c} = 6 + \frac{R_{ck} - 15}{4} \tag{1}$$

$$f_{ctm} = 0.27\sqrt[3]{R_{ck}^2} \tag{2}$$

where $\sigma_{adm,c}$ represents the admissible compressive strength while f_{ctm} is the average tensile strength. In the formulas, R_{ck} is the characteristic compressive strength that, substantially, constitutes the fifth percentile of all strengths. It has the probability of not being exceeded equal to 5%. Due to a lack of information, assuming an R_{ck} equal to 30 MPa, the reference values prescribed by Eqs. (1) and (2) are the following: $\sigma_{adm,c} = 9.75$ MPa and $f_{ctm} = 2.61$ MPa. So, Table 4 reports the maximum percentage ratios between the tensile and compression tensions and their admissible values for each spectrum direction, in both empty and filled configurations. The results show how the compression tensions work for percentages below the 10% respect the admissible one.

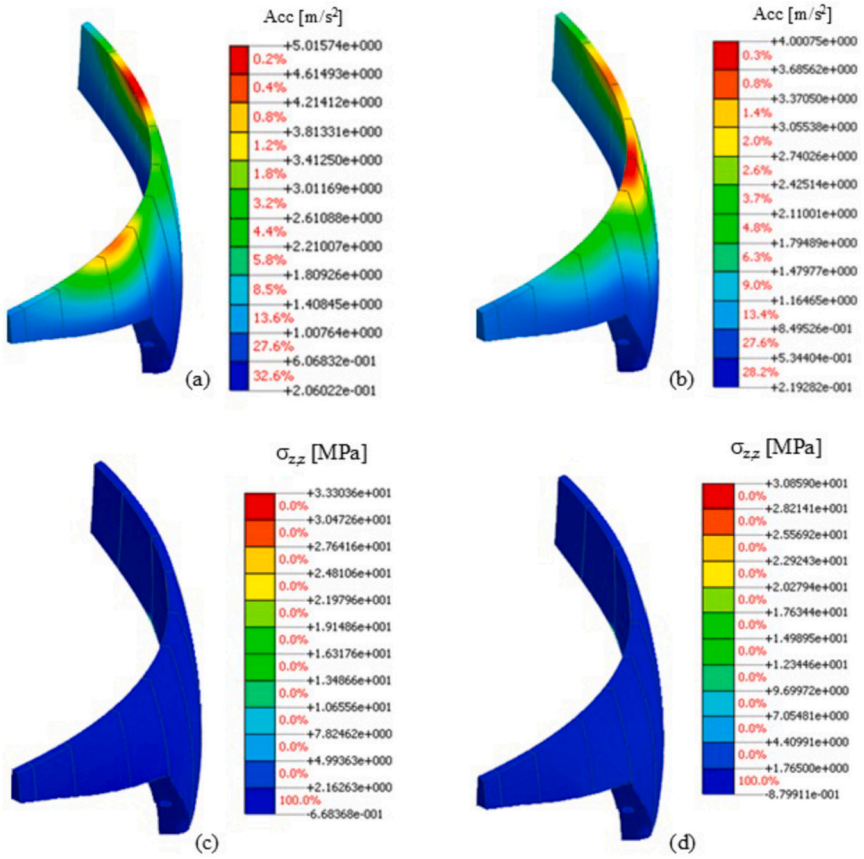

Fig. 12. Response spectrum analysis: acceleration distributions for X' (a) and Y (b) direction and normal tension in z-direction distributions for X' (c) and Y (d) direction (see Fig. 7c). Filled configuration.

Table 4
Material working rate (compression and tension) [$\sigma_{x,x}$, $\sigma_{y,y}$, $\sigma_{z,z}$] for different spectrum directions.

Spectrum direction	Empty dam		Filled dam	
	Compression (%)	Tensile (%)	Compression (%)	Tensile (%)
X	6.08	39.51	6.15	52.17
Y	9.02	67.52	3.08	83.24
X'	6.40	80.17	6.87	82.86
Y'	9.74	21.10	9.85	18.41

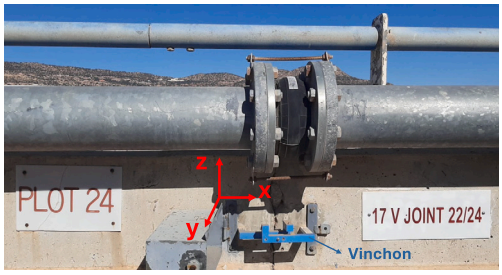

Fig. 13. Displacement measurement system based on vinchons (or winches).

Instead, the tensile ones are widely higher, but in any case, they do not overcome the corresponding average tensile strength. Based on these results, the following observations can be drawn:

- A basic setup for a seismic structural health monitoring system might include three accelerometers placed at the top of the dam: one at a quarter length, one at half length, and one at three-quarters length.
- Such sensors must be able to measure an acceleration peak at least equal to 0.50 g.
- The computational model prediction shows substantially a linear behavior with a tensional scenario below admissible values if a seismic input induces a maximum response below 0.50 g.

4. Dam behavior during 2023 Marrakech-Safi Earthquake

On 8 September 2023, at 23:11 local time, a 6.8 magnitude earthquake struck the Marrakech-Safi region in northwestern Morocco. The earthquake was felt not only in Morocco but also in Spain, Portugal, and Algeria. It destroyed several villages near the epicenter and caused significant damage to buildings in other parts of the country, causing the collapse of some structures. The province of Al Haouz, where the epicenter was located, was the hardest hit area, but the consequences of the earthquake were also severe in Marrakech, as well as in the provinces of Ouarzazate, Azilal, Chichaoua, and Taroudant. The World Health Organization estimates that around 300,000 people have been affected in Marrakech and its surrounding areas. This was the most powerful earthquake ever recorded in Morocco and the deadliest earthquake to date in the country.

The measured seismic wave of 2023 Marrakech-Safi Earthquake has been downloaded from the RTC station (located in Rabat, Morocco) belonging to the Mediterranean Very Broadband Seismographic Network (https://doi.org/10.13127/SD/FBBBTDTD6Q). In particular, the channels HHE (East-West direction), HHN (North-South direction) and HHZ (Vertical direction) have been retrieved. Moreover, this Station is managed by the National Institute of Geophysics and Volcanology (in Italian Istituto Nazionale di Geofisica e Vulcanologia, INGV, http://terremoti.ingv.it/instruments/station/RTC). It is right to highlight that the sensors installed in the RTC Station are velocimeters that mea-

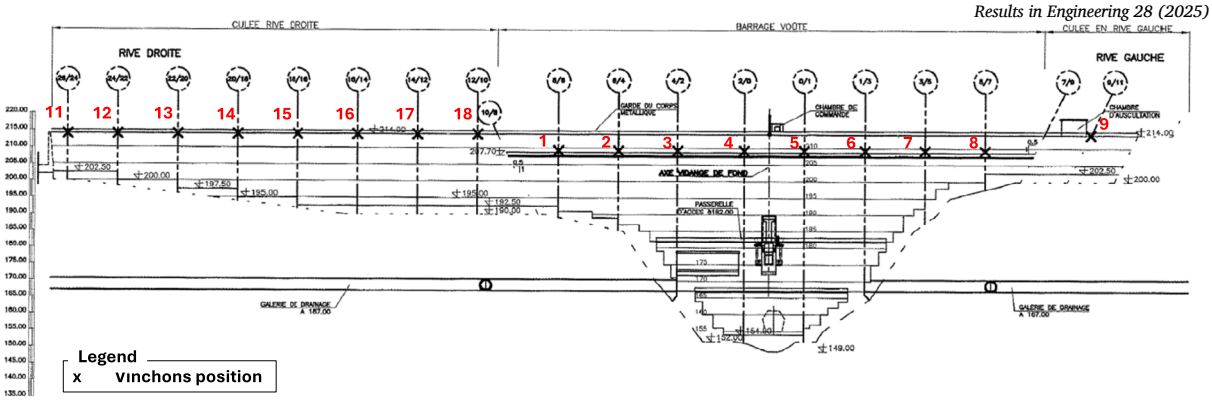

Fig. 14. Layout of vinchons, longitudinal view of the dam from downstream.

sure the seismic ground acceleration in counts. So, the measurements, first, have been converted in m/s^2 units, dividing by the sensitivity, then have been applied a detrend remove and, finally, the time history has been differentiated to obtain the accelerations. Based on the values of PGA distributed in the different regions of Morocco during the 2023 Marrakech-Safi Earthquake (source USGS: https://earthquake.usgs.gov/earthquakes/eventpage/us7000kufc/executive), the accelerometric recorded data have been amplified to simulate the accelerations on the epicenter (factor of amplification about equal to PGA(RTC Station) / PGA(Marrakesh) = 0.5000 g / 0.0351 g = 14.2348) and then they have been deamplified to simulate the accelerations had on Dam site (factor of deamplification about equal to PGA(Marrakesh) / PGA(Dam site) = 0.50 g / 0.05 g = 10.0). The time history in East-West direction (that it was almost only in North-South direction) and the corresponding spectrum, evaluated considering a damping ratio equal to 5%, have been reported in the Fig. 11c,d, respectively. More information on seismic hazard assessment in the country of North Africa can be found in [36].

During the earthquake, the behavior of the dam has been observed using the displacement measurement system based on vinchons (or winches), shown in Fig. 13, applied to monitor the movement or deformation of the dam structure over time and measure joint openings. It is right to highlight that during an inspection, carried out in August 2023, no major damage on the dam was detected.

This displacement monitoring system is vital for ensuring the structural integrity of the dam, as it helps identify changes or problems that might not be immediately visible but could lead to more serious problems if left unchecked. The vinchon-based displacement measurement system involves the use of winches, which are mechanical devices anchored to specific points of the dam structure. These winches are typically installed at strategic locations, such as the crest, abutments, or across the joints of the dam, where monitoring displacements and joint opening could occur. The Prince Moulay Abdellah Dam is equipped with 17 vinchons whose layout is shown in Fig. 14: 8 vinchons installed on the vault (V1-V8), 1 on the left abutment (V9), and 8 on the right abutment (V11-V18).

The vinchon measurements acquired during August and September 2023 are reported in Fig. 15. The red line in the graph indicates the date of the earthquake. The displacement measurements are shown in three directions: the x-direction represents the longitudinal direction (from shore to shore, tangential to the dam profile), the y-direction represents the transverse direction (from upstream to downstream, perpendicular to the dam profile), and the z-direction represents the vertical direction. The data reveal a distinct behavior between the dam's abutments and its vault. For the abutments, the absolute displacement values increase after the earthquake, particularly in the x-direction (longitudinal), and to a lesser extent in the y-direction (transverse). In contrast, the measurements for the vault show a nearly constant trend, with little variation before and after the seismic event.

To better illustrate the variation in displacements following the seismic event, the mean value of displacements before ($\overline{d}_0$) and after ($\overline{d}_e$) the earthquake was calculated (Fig. 16 a,c,e). Then, the mean value variation was computed (Fig. 16b,d,f) as follows:

$$\Delta\overline{d} = \frac{\overline{d}_e - \overline{d}_0}{\overline{d}_0}, \tag{3}$$

removing outlier values such as the case of measure V15Z (see Fig. 15f). The plots shown in Fig. 16 highlight that while the vault (measurement points V1-V8) exhibits higher displacement values, the variation in displacement after the earthquake is greater for the abutments (measurement points V11-V18).

The monitoring data acquired close to the seismic event highlight the differences in behavior at various points of the dam, providing insights into how the dam's structure responded to the seismic activity. It can be concluded that the dam's abutments exhibited a more earthquake-sensitive behavior. This is likely since the vault has been reinforced to a greater extent, as it represents the main body of the dam.

The small displacements recorded by the winches indicate that the dam remained in the elastic range during the earthquake. To confirm this, a response-spectrum analysis was repeated using the spectrum derived from the ground accelerations measured at the RTC station. As shown in Fig. 17, the resulting stresses are highly localized, with peak values concentrated in the $\sigma_{z,z}$ component, both in tension and compression. This distribution closely matches that obtained with the design spectrum prescribed by the Italian code NTC-08 (Fig. 11b). In both cases the effective peak acceleration is about 0.50 g. The corresponding maximum tensile and compressive stresses are approximately 12% and 85% of the allowable limits, respectively, confirming that the dam's response remains safely within the elastic domain.

5. Conclusions

The study highlights the importance of advanced computational modeling and monitoring techniques in ensuring the safety and structural integrity of critical infrastructures such as the Prince Moulay Abdellah Dam, particularly in seismically active regions like Agadir, Morocco. By integrating BIM, FEM analysis, and real-time monitoring data, a comprehensive framework has been developed to assess the dam's structural behavior under seismic loads.

The application of BIM in FEM modeling has proven to be particularly effective due to its interoperability capabilities, facilitating seamless data exchange between different computational environments. Furthermore, BIM enables efficient management of monitoring system data, providing an intuitive and structured representation of sensor information. This study underscores BIM's potential to transform the design, monitoring, and maintenance of hydraulic infrastructures, paving the way for a more integrated and proactive management approach. By

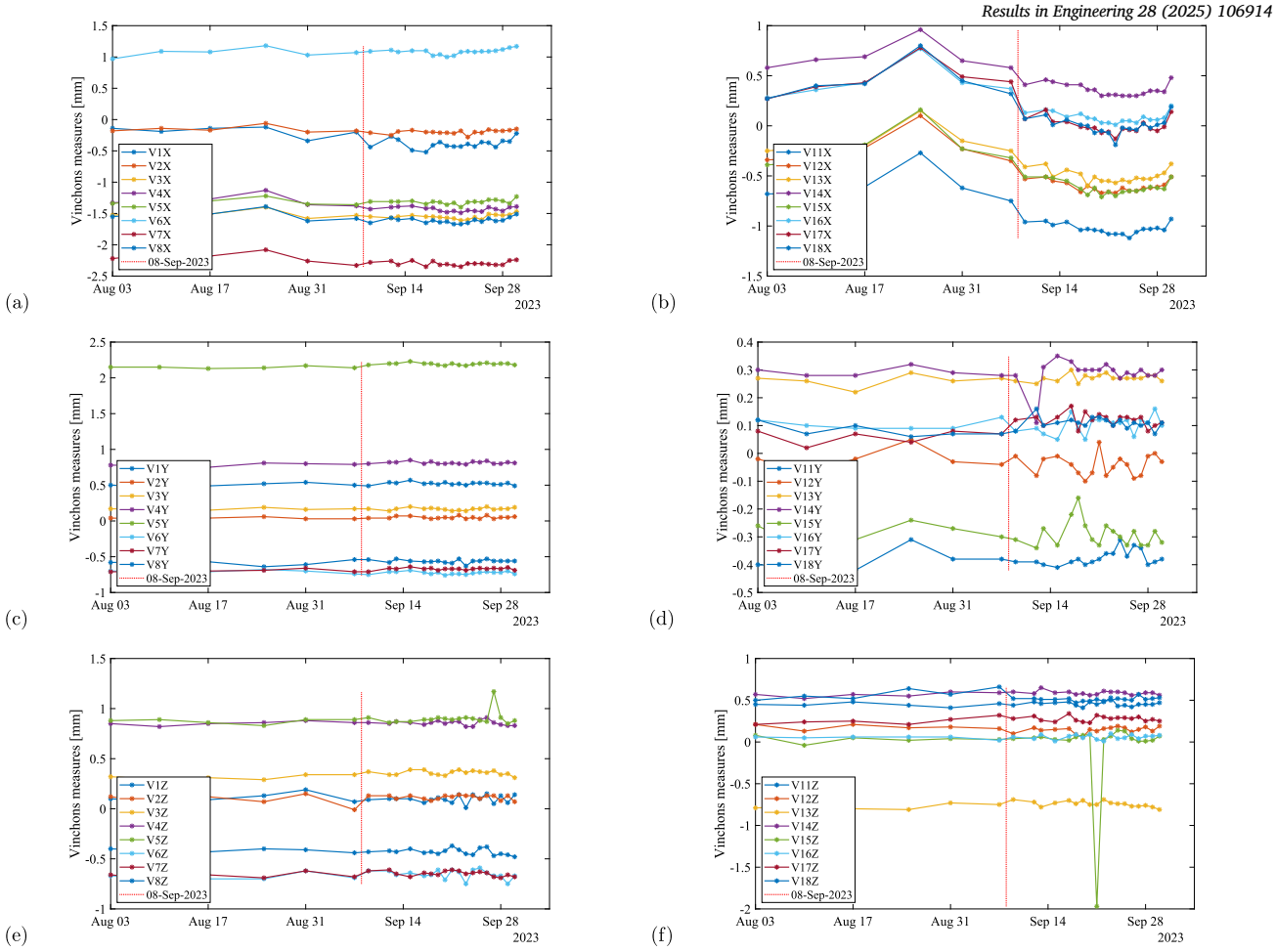

Fig. 15. Measures of vinchons installed on the vault (a,c,e) and on the abutments (b,d,f) in x (a,b), y (c,d), and z (e,f) direction. The vertical red line corresponds to the Marrakesh-Safi earthquake.

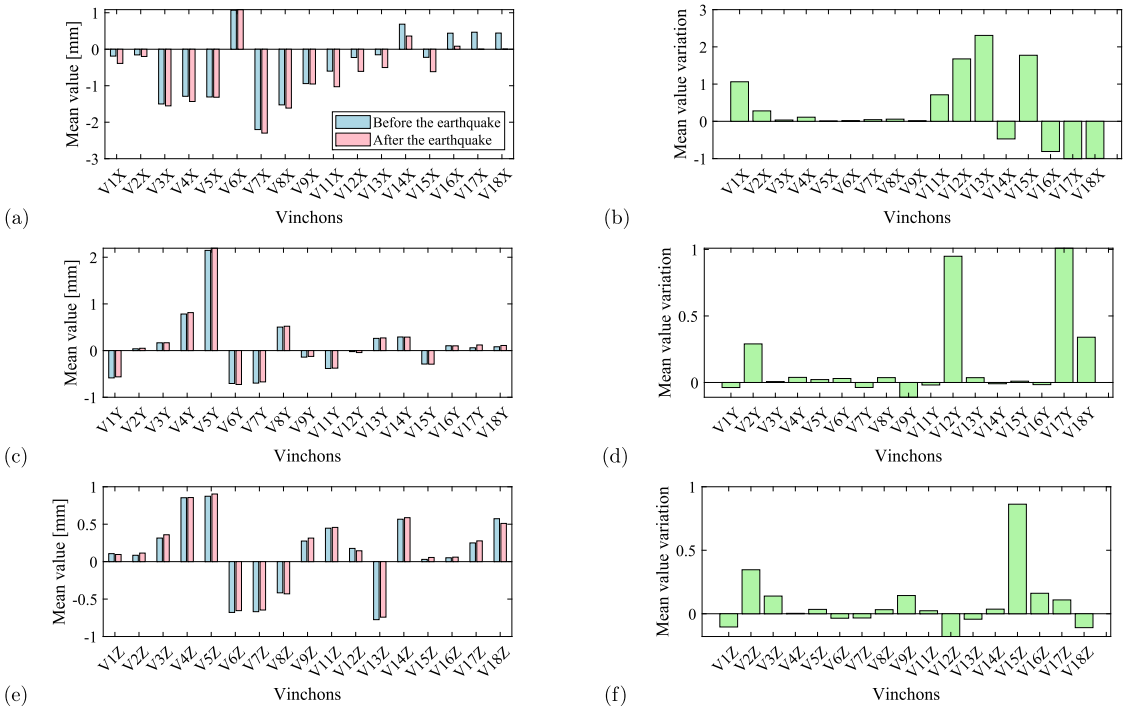

Fig. 16. Mean of displacements before and after the earthquake (a,c,e) and mean variation (b,d,f) in x (a,b), y (c,d) and z (e,f) direction.

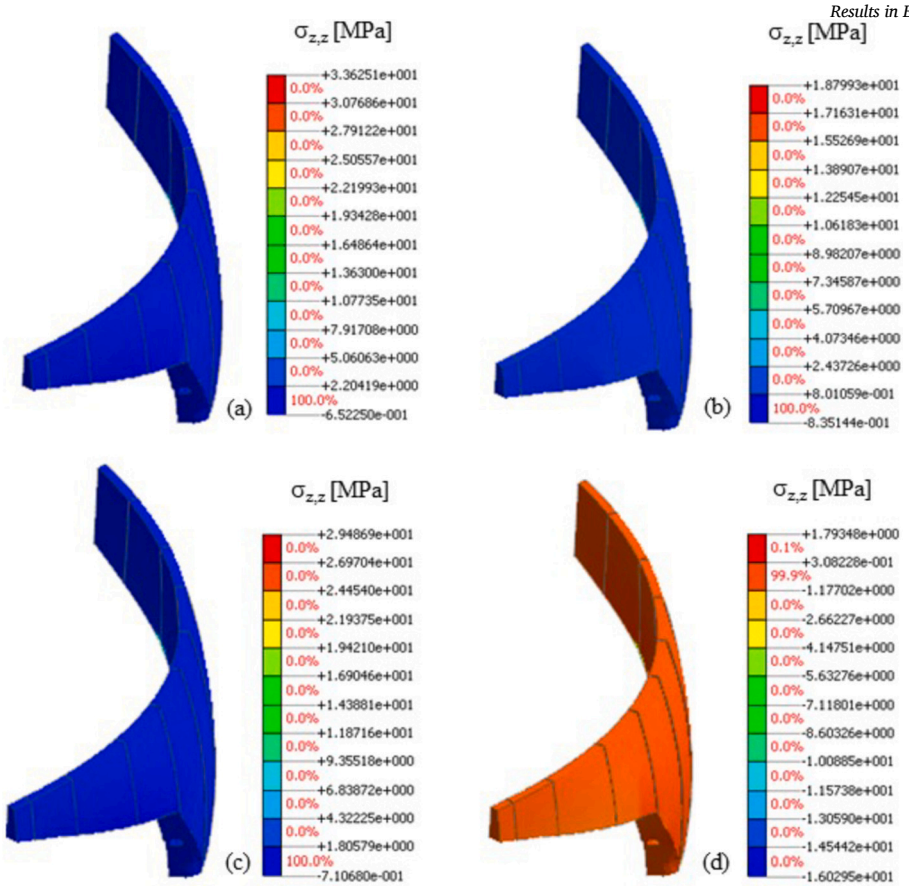

Fig. 17. Response spectrum analysis using the input evaluated from RTC Station measurements (Fig. 11d): tensions $\sigma_{z,z}$ for empty (a,b; X' and Y' direction, respectively) and filled (c,d; X' and Y' direction, respectively) configurations.

leveraging complex datasets, decision-making in risk assessment and emergency planning can be significantly improved.

The development of a 3D computational model, based on BIM-generated information and on-site experimental data, has demonstrated its utility in optimizing the placement of monitoring sensors and defining accelerometric thresholds to ensure the linear dynamic behavior of the arch dam. Additionally, this model serves as a foundation for advanced nonlinear simulations, enabling the prediction of stress scenarios under extreme seismic loads.

The seismic response observed by the dam during the earthquake of September 8, 2023 provided key insights into its structural performance. Displacement measurements revealed that the abutments exhibited a more pronounced longitudinal response compared to the vault, which remained relatively stable. This difference is likely due to the greater reinforcement of the vault, as it constitutes the primary structural element of the dam. The joints between concrete blocks performed within acceptable safety margins, further confirming the resilience of the dam under seismic excitation.

In conclusion, the methodologies presented in this study contribute to a deeper understanding of dam seismic resilience and emphasize the importance of integrating advanced technologies in the ongoing monitoring and management of hydraulic structures. Future research should focus on expanding the application of BIM-FEM methodologies (especially aiming to improve the automatic interoperability) to other dams and hydraulic infrastructures, refining predictive models (for instance, by offering a more thorough characterization of the nonlinear fracture mechanisms, especially those occurring at joint regions), and enhancing early warning systems to better anticipate and mitigate seismic risks. The continued evolution of digital modeling and real-time monitoring tools will play a crucial role in safeguarding water resources and protecting downstream communities in earthquake-prone regions.

CRediT authorship contribution statement

Cecilia Rinaldi: Writing – original draft, Formal analysis. **Amine Bendarma:** Visualization, Data curation. **Francesco Potenza:** Writing – review & editing, Validation. **Vincenzo Gattulli:** Funding acquisition, Conceptualization.

Funding

The research has been supported by IRIS Project financed by the NATO Science for Peace and Security Programme under grant id. G5924 and the Italian Project TECNODIGIT funded by the European Union – NEXT GENERATION EU – Research Program ROME TECHNOPOLE Project code ECS 00000024 - Spoke 1 e 6.

Declaration of competing interest

The authors declare that they have no known competing financial interests or personal relationships that could have appeared to influence the work reported in this paper.

Acknowledgements

The authors would like to express their special thanks to Hamza Elhimri, an engineer at the Souss Massa Hydraulic Basin Agency, and Hamza Bouchta for their valuable contributions and assistance throughout the study. The authors would also like to thank the Laboratory for Sustainable Innovation and Applied Research at Universiapolis - International University of Agadir, where Amine Bendarma worked during the development of the NATO IRIS project, in which he served as co-PI. Finally, the authors would like to thank the students Lisa Caroso

(University “G. d’Annunzio” of Chieti-Pescara) and Cecilia Mastroiacovo (Sapienza University of Rome) for their assistance in implementing the 3D computational models and BIM model, respectively.

Data availability

The authors do not have permission to share data.

References

[1] G. Prakash, A. Sadhu, S. Narasimhan, J.-M. Brehe, Initial service life data towards structural health monitoring of a concrete arch dam, Struct. Control Health Monit. 25 (1) (2018) 2036.

[2] X. Zhu, J. Qiu, Y. Xu, X. Chen, P. Xu, X. Wu, S. Guo, J. Zhao, J. Lin, Modal parameter recursive estimation of concrete arch dams under seismic loading using an adaptive recursive subspace method, Sensors 24 (12) (2024) 3845.

[3] M.-Z. Zhang, L. Zhang, X.-C. Wang, W. Su, Y.-X. Qiu, J.-T. Wang, C.-H. Zhang, A framework for seismic response analysis of dams using numerical source-to-structure simulation, Earthq. Eng. Struct. Dyn. 52 (3) (2023) 593–608.

[4] S. Pereira, F. Magalhães, J.P. Gomes, Á. Cunha, J.V. Lemos, Dynamic monitoring of a concrete arch dam during the first filling of the reservoir, Eng. Struct. 174 (2018) 548–560.

[5] S. Oliveira, A. Alegre, E. Carvalho, P. Mendes, J. Proença, Seismic and structural health monitoring systems for large dams: theoretical, computational and practical innovations, Bull. Earthq. Eng. 20 (9) (2022) 4483–4512.

[6] M. Venugopal, C.M. Eastman, R. Sacks, J. Teizer, Semantics of model views for information exchanges using the industry foundation class schema, Adv. Eng. Inform. 26 (2) (2012) 411–428.

[7] A. Løkke, A.K. Chopra, Direct finite element method for nonlinear earthquake analysis of concrete dams: simplification, modeling, and practical application, Earthq. Eng. Struct. Dyn. 48 (7) (2019) 818–842.

[8] M.K. Anari, S.M. Mirhosseini, S.H. Lajevardi, E. Zeighami, Effect of foundation stiffness on the fragility curves of a concrete gravity dam under far-field ground motions, Results Eng. 24 (2024) 102962.

[9] M. Colombo, M. Domaneschi, A. Ghisi, et al., Existing concrete dams: loads definition and finite element models validation, Struct. Monit. Maint., Int. J. 3 (2) (2016) 129–144.

[10] C. Rinaldi, A. Talebi, M. D’Alessio, F. Potenza, V. Gattulli, Identification of natural and forcing frequencies through noisy measurements acquired in operational conditions on a hospital building, Adv. Civ. Eng. 2024 (1) (2024) 4447739.

[11] M. Crognale, C. Rinaldi, F. Potenza, V. Gattulli, A. Colarieti, F. Franchi, Developing and testing high-performance shm sensors mounting low-noise mems accelerometers, Sensors 24 (8) (2024) 2435.

[12] B. Beiranvand, T. Rajaee, M. Komasi, Spatiotemporal clustering of dam settlement monitoring using instrumentation data (case study: Eyvashan Earth Dam), Results Eng. 22 (2024) 102014.

[13] R. Zhu, T. Guo, L. Song, K. Yang, G. Xu, S. Tesfamariam, Seismic vulnerability assessment of self-centering prestressed concrete frames with and without masonry infill walls: experimental and numerical models, J. Struct. Eng. 150 (8) (2024) 04024087.

[14] J.P. Gomes, J.V. Lemos, Characterization of the dynamic behavior of a concrete arch dam by means of forced vibration tests and numerical models, Earthq. Eng. Struct. Dyn. 49 (7) (2020) 679–694.

[15] S. Alves, J. Hall, System identification of a concrete arch dam and calibration of its finite element model, Earthq. Eng. Struct. Dyn. 35 (11) (2006) 1321–1337.

[16] X. Cao, L. Chen, J. Chen, J. Li, W. Lu, H. Liu, M. Ke, Y. Tang, Seismic damage identification of high arch dams based on an unsupervised deep learning approach, Soil Dyn. Earthq. Eng. 168 (2023) 107834.

[17] T.-Y. Hsu, C.-H. Loh, Damage detection accommodating nonlinear environmental effects by nonlinear principal component analysis, Struct. Control Health Monit., Off. J. Int. Assoc. Struct. Control Monit. Eur. Assoc. Control Struct. 17 (3) (2010) 338–354.

[18] C.-H. Loh, C.-H. Chen, T.-Y. Hsu, Application of advanced statistical methods for extracting long-term trends in static monitoring data from an arch dam, Struct. Health Monit. 10 (6) (2011) 587–601.

[19] R. Zhu, T. Guo, T. Xie, T. Xu, K. Deng, G. Xu, S. Tesfamariam, Seismic design of self-centering prestressed concrete frames with sliding infill walls: parameter analysis and seismic demand prediction, Eng. Struct. 335 (2025) 120346.

[20] R. Zhu, T. Guo, S. Hu, T. Wang, Y. Xia, S. Tesfamariam, Probabilistic seismic design method for high-rise self-centering friction-viscous braced steel moment-resisting frames using the xgboost-ga algorithm, Thin-Walled Struct. 215 (2025) 113394.

[21] O.M. Sorkhabi, B. Shadmanfar, E. Kiani, Monitoring of dam reservoir storage with multiple satellite sensors and artificial intelligence, Results Eng. 16 (2022) 100542.

[22] M. De Iuliis, M. Crognale, F. Potenza, V. Gattulli, On the combined use of satellite and on-site information for monitoring anomalous trends in structures within cultural heritage sites, J. Civ. Struct. Health Monit. 14 (5) (2024) 1173–1190.

[23] Y. Zhou, T. Bao, X. Shu, Y. Li, Y. Li, Bim and ontology-based knowledge management for dam safety monitoring, Autom. Constr. 145 (2023) 104649.

[24] Y. Fang, S.-A. Mitoulis, D. Boddice, J. Yu, J. Ninic, Scan-to-bim-to-sim: automated reconstruction of digital and simulation models from point clouds with applications on bridges, Results Eng. 25 (Mar 2025) 104289.

[25] I. Khadrouf, O. El Hammoumi, N. El Goumi, M. Oukassou, Contribution of hvsr, masw, and geotechnical investigations in seismic microzonation for safe urban extension: a case study in Ghabt Admin (Agadir), western Morocco, J. Afr. Earth Sci. 210 (2024) 105138.

[26] S. Bruno, M. De Fino, F. Fatiguso, Historic building information modelling: performance assessment for diagnosis-aided information modelling and management, Autom. Constr. 86 (2018) 256–276.

[27] A. Barontini, C. Alarcon, H.S. Sousa, D.V. Oliveira, M.G. Masciotta, M. Azenha, Development and demonstration of an hbim framework for the preventive conservation of cultural heritage, Int. J. Archit. Herit. 16 (10) (2022) 1451–1473.

[28] M.L. Leonardi, J. Granja, D.V. Oliveira, M. Azenha, Scalable bim based open workflow for structural analysis of masonry building aggregates, Comput. Struct. 297 (2024) 107321.

[29] Y. Fang, S.-A. Mitoulis, D. Boddice, J. Yu, J. Ninic, Scan-to-bim-to-sim: automated reconstruction of digital and simulation models from point clouds with applications on bridges, Results Eng. 25 (2025).

[30] A.B. Mohammed, Applying bim to achieve sustainability throughout a building life cycle towards a sustainable bim model, Int. J. Constr. Manag. 22 (2) (2022) 148–165.

[31] B. Habte, E. Guyo, Application of bim for structural engineering: a case study using Revit and customary structural analysis and design software, J. Inf. Technol. Constr. 26 (2021) 1009–1022.

[32] K.O. Cetin, B.U. Ayhan, F. Cüceoğlu, S. Yildirim, Performance of Reyhanlı Dam during February 6, 2023 Kahramanmaraş-Türkiye earthquake sequence, Soil Dyn. Earthq. Eng. 194 (2025) 109369.

[33] S. Ji, T. Hu, Construction Simulation and Real-Time Monitoring Research of Concrete Dam Based on Bim, IOP Conference Series: Earth and Environmental Science, vol. 304, IOP Publishing, 2019, 052056.

[34] R.E. Goodman, Introduction to Rock Mechanics, 2nd edition, John Wiley & Sons, 1991.

[35] T. Waltham, Foundations of Engineering Geology, 2nd edition, CRC Press, 2002.

[36] T. Mourabit, K.M. Abou Elenean, A. Ayadi, D. Benouar, A. Ben Suleman, M. Bezzeghoud, A. Cheddadi, M. Chourak, M.N. ElGabry, A. Harbi, M. Hfaiedh, H.M. Hussein, J. Kacem, A. Ksentini, N. Jabour, A. Magrin, S. Maouche, M. Meghraoui, F. Ousadou, G.F. Panza, A. Peresan, N. Romdhane, F. Vaccari, E. Zuccolo, Neodeterministic seismic hazard assessment in North Africa, J. Seismol. 18 (2) (2014) 301–318.